Ultrasonic Evaluation of Spot Weld Quality

Agreement between experimental results and theoretical predictions indicates ultrasonic measurement of nugget diameter may be a valid method of predicting shear strength of spot welds

BY S. I. ROKHLIN AND L. ADLER

ABSTRACT. A novel ultrasonic method for evaluation of shear strength of a spot weld is discussed. This method is based on an analytical expression which relates the transmission coefficient of Lamb waves passing through a spot weld nugget to the nugget diameter. The use of an ultrasonic spectroscopic method for determining nugget size is also discussed.

A fracture mechanics model is introduced to correlate fracture load to the nugget dimension. This model predicts that the failure load is proportional to the squared nugget diameter. While the model is valid only when the weld fails through the nugget, it was shown experimentally that the proportionality of the failure load to the square of the diameter holds also when the failure occurs in the base metal.

When the ultrasonic Lamb wave transmission coefficient is measured through spot welds and related to fracture load, there is good agreement between experimental results and model predictions. It appears ultrasonic waves can be used to estimate shear strength of spot welds.

Introduction

The major aim of nondestructive evaluation of materials is quantitative prediction of their mechanical properties. For a given material structure the quantitative information on flaws found by NDT methods can be used for strength prediction using methods of fracture mechanics. In this paper, we use such concepts for evaluation of spot welds. We use ultrasonic techniques for sizing spot weld diameters, and based on ultrasonic data, we develop a fracture mechanics model for prediction of failure load.

Recently (Refs. 1, 2), a new ultrasonic Lamb wave technique was proposed and checked for sizing of spot welds. According to this technique, the spot weld was modeled by a circular aperture which acoustically coupled two welded sheets. The welded region is common to both sheets, whereas in the outside region the sheets are separated by infinite slits opaque to elastic waves. The effect of penetration of elastic waves from one plate to another through the coupling region can be used to estimate the dimension of the welded region (weld nugget). The diameter of the weld nugget is an important factor for evaluating the failure load of the welded joint.

The goal of this paper is to discuss the further development of this new ultrasonic method and to relate ultrasonic measurements to weld strengths. We study spot welds with relatively small nugget diameters for which failure occurs through the nugget. The case of welds with large nugget sizes was considered by us elsewhere (Ref. 3), where ultrasonic methods were applied for on-line monitoring and strength prediction of spot welds.

This paper will review some results of Ref. 1 for the Lamb wave transmission coefficient, and discuss the application of the leaky Lamb wave in immersion techniques. Furthermore, we discuss a fracture mechanics model for the same problem and its relation to ultrasonic methods, and then describe the experimental technique and present discusssion of the experimental results.

S. I. ROKHLIN is a professor in the Materials Engineering Department, Ben-Gurion University of the Negev, Beer-Sheva, Israel. L. ADLER is Professor of Welding Engineering and Engineering Mechanics, The Ohio State University, Columbus, Ohio.

Explanation of the Method and Theoretical Model

Determination of the Spot Diameter

The main idea of the method of measurements is illustrated schematically in Fig. 1A. The Lamb wave, excited in the upper sheet, is incident onto the welded region. The incident energy is partially reflected, but most of the energy is passed into the lower sheet and is detected by the receiving transducer. The value of the transmission coefficient must characterize the dimensions of the welded region.

To understand the interaction of the Lamb wave with the welded region, consider the two dimensional model shown schematically in Fig. 2. A wave is incident from region I onto the sheet junction region III. The incident wave is partially reflected back into region I from the tip of the slit L_1 and, being additionally diffracted at this tip, turns into region I. This diffraction can be treated as a diffraction at a semi-infinite slit (Ref. 1). Most of the energy of the incident wave passes into region III of the junction between the sheets, transforming into those modes which are possible there, with amplitude transformation coefficients D_{in} (i is the number of the incident wave, and n is the number of one of the modes generated in region III).

We shall clarify the above by means of dispersion curves (Refs. 4, 5) for propagating Lamb waves, as shown in Fig. 3. Here $K_t h = 2\pi fh/C_t$ is shown on the

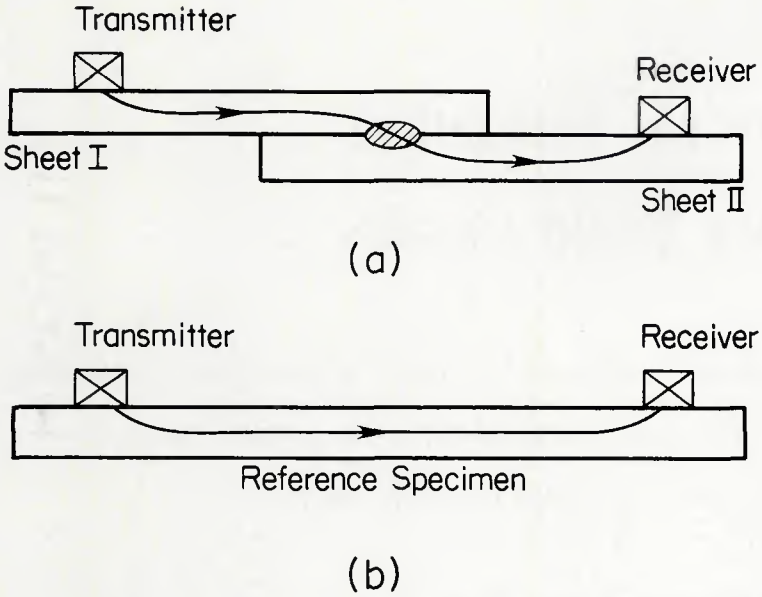

Fig. 1—Schematic illustration of the method of measurements. A—welded specimen; B—reference

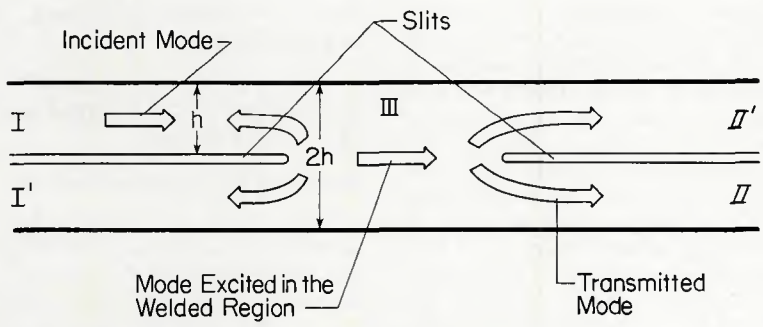

Fig. 2—Schematic explanation of Lamb wave diffraction by aperture

abscissa axis, where f is the frequency, h is half the layer thickness, and C_t is the velocity of the shear wave for the material of the layer. The calculations were performed for steel, where it is assumed that the Poisson ratio $\nu = 0.292$. The nondimensional wavenumber $\alpha = K/K_t = C_t/V$, where V is the phase velocity of the corresponding Lamb wave and K is its wavenumber, is shown on the ordinate axis. If, for example, the frequency is such that $K_t h$ for the regions I, I′, II, and II′ is equal to 2, then modes S_o, A_1, and A_o may propagate there. In the region of joining of the plates (region III), the thickness is double, and hence $K_t h = 4$. At this value of $K_t h$, modes S_2, S_1, A_1, S_o, and A_o may propagate.

The propagating waves generated in the region where the plates are joined are multiply reflected from the tips of the slits. In the course of these oscillations, waves are radiated from region III into regions I, I′, II, and II′ with formation of transmitted and reflected fields.

In addition to the above propagating waves, an infinite set of nonpropagating waves is excited, consisting of a finite number of waves with purely imaginary wavenumbers and an infinite number of waves with complex wavenumbers. These modes make their contribution primarily near edges L_1 and L_2 in such a manner that conditions at the edge associated with a concentration of elastic stresses are satisfied (Ref. 6).

The resonance properties of the diffracted field are determined by coefficients of reflection from the edges of the slits in the cavity region. It was shown in Ref. 6 that to be able to estimate the resonance properties it suffices to consider the single-mode approximation. In this approximation, the conditions for resonance are obtained by requiring that the function

$$|1 \pm |R_{nn}| \exp(iK_n L + \phi_{nn})| = [1 + |R_{nn}^2| \pm 2|R_{nn}| \cos(K_n L + \phi_{nn})]^{1/2} \quad (1)$$

be at a minimum. For the first resonance, we have

$$L = \lambda/2 - \phi_{nn}\lambda/(2\pi), \quad (2)$$

where ϕ_{nn} is a phase correction associated with the radiation from the cavity. It is seen that the resonance can be avoided when all the reflection coefficients R_{nn} in the inner region of the cavity become zero.

It was shown by Rokhlin that at $K_t h = \sqrt{2}\,\pi$, all the reflection coefficients associated with the incident mode A_1 become zero. The wavenumber for mode A_1 in this point is obtained from the condition that $2K^2 - K_t^2 = 0$; hence, we have $V_L = \sqrt{2}\,V_t$ for the velocity. The Lamb wave at this point is the Lamé mode (Ref. 4). The latter is a pure shear wave SV propagating at an angle of 45° to the surface of the plate. At this angle, there is no mutual transformation of shear to longitudinal waves on the free solid surface. To satisfy the Lamé mode conditions in the welded region, it is necessary to excite incident mode S_o at a frequency such that, for a given thickness h of the sheets being joined, we will obtain $K_t h = \pi\sqrt{2}$.

All the above can be extended to the three-dimensional case of a circular aperture. In this case the quantity of transmitted energy also depends on the size of the region in the direction perpendicular to that of the wave. The conditions for radial resonances are analogous to equation (1). In our case, for the selected conditions (mode S_o), there will be no pronounced radial resonances in the region of the aperture.

In the case of absence of resonance in the aperture region, a one-to-one correspondence will exist between the diameter of the aperture and the coefficient of transmission of mode S_o from the region I to region II. Therefore, the solution of the inverse problem of finding the dimension of the aperture from the amplitude of the transmitted wave seems particularly simple.

It has been previously shown (Ref. 1) that the particular case under consideration of scattering of the Lamé mode can be reduced approximately to the problem of scattering of scalar waves. Since the incident field is specified only in region I, while being equal to zero in region II, the displacement component in the incident wave undergoes a jump in the plane of the aperture (the components of the stress tensor of the incident field in this plane are equal to zero). Since the total displacement field in the plane of the aperture should be continuous, breaks in the incident field are compensated by discontinuities of the diffraction field. The discontinuity in the diffracted field corresponds to the presence of field

sources in the plane of the aperture. Hence, only normally oriented displacement sources form in the plane of the aperture. The field in the aperture region also forms basically as the Lamé mode (mode A_1). We, then, assume approximately that an incident SV wave is not transformed into a longitudinal wave. In this approximation, the elastic problem reduces to a scalar problem and the incident u^i and transmitted u^t displacement fields are specified for the S_o wave in the form

$$u_y^i = A_i(K_t/2)\sin(\pi y/h);$$
$$u_y^t = A_iT(K_t/2)\sin(\pi y/h),$$
$$u_z^i = A_i(\pi/h)\cos(\pi y/h);$$
$$u_z^t = A_iT(K_t/2)\cos(\pi y/h). \quad (3)$$

The y coordinate is perpendicular to the plate surface; T is the coefficient of transmission from region I to region II. A is a normalizing coefficient in the incident wave, with dimensions cm^2. In this formulation, the problem is fully identical to that of coupling between two electromagnetic waveguides through a small aperture, considered by Collin (Ref. 8), with the only difference being that a normally oriented dipole forms in the region of the aperture. In the case of a small circular aperture (Ref. 1), we obtain

$$T \sim K_t h(d/h)^3. \quad (4)$$

The dependence on $(d/h)^3$ is satisfied at $d < h$. In the case where the size of the aperture becomes comparable with the wavelength, it starts exhibiting resonant properties.

In our case, the coupling aperture cannot be regarded as small compared with the wavelength. However, the parameter $K_t h$ was selected in such a manner that the resonance properties of the aperture are not realized. It can hence be assumed that equation (4) holds also at $d \sim h$.

By virtue of the simplicity of the relationship between the amplitude of the transmitted wave and the diameter of the junction region, one can naturally solve the inverse problem of determining the mean diameter of the weld region on the basis of the amplitude of the transmitted wave. Here, given that $d \sim (T)^{1/3}$, the method is not sensitive to experimental errors. This allows direct determination of the mean diameter which is related to the strength of the joint.

If the tested samples are immersed in liquid, then propagating Lamb waves become leaky waves, due to leakage of the elastic energy from the plate to the liquid (the angle of leakage can be determined according to Snell's law). The situation is shown schematically in Figs. 4A and 4B. We must distinguish two cases: the case with an air gap between the sheets (Fig. 4A), and the case with a liquid filled gap between the sheets — Fig. 4B. In the first case, the situation changes only slightly from the nonimmersion case considered above — Fig. 2. A leaky Lamb wave is incident onto the junction region (III) and is partially transmitted into region II. The velocity of the leaky Lamb wave is only slightly different from the velocity of the usual Lamb wave (Ref. 5) and, therefore, the transmission process through the diaphragm does not change. The only difference is that there is a small field scattered into the liquid (shown in broken lines in Fig. 4A). It must be pointed out

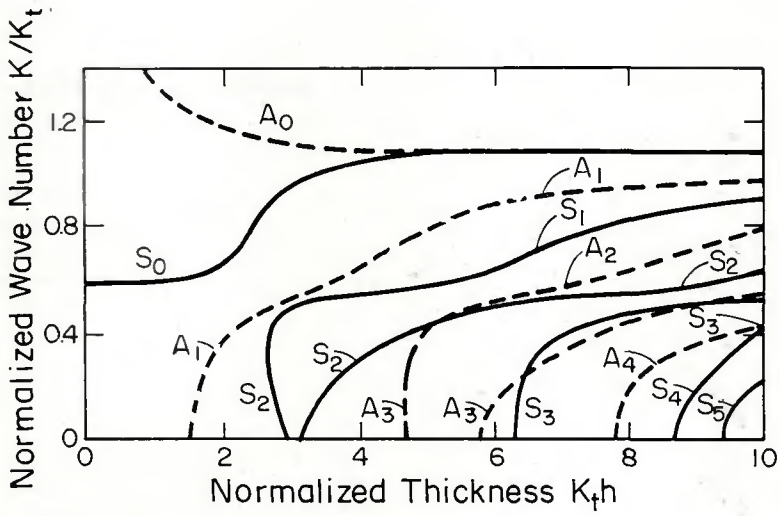

Fig. 3 — Dispersion curves for the real wave numbers of the propagating wave (data for steel)

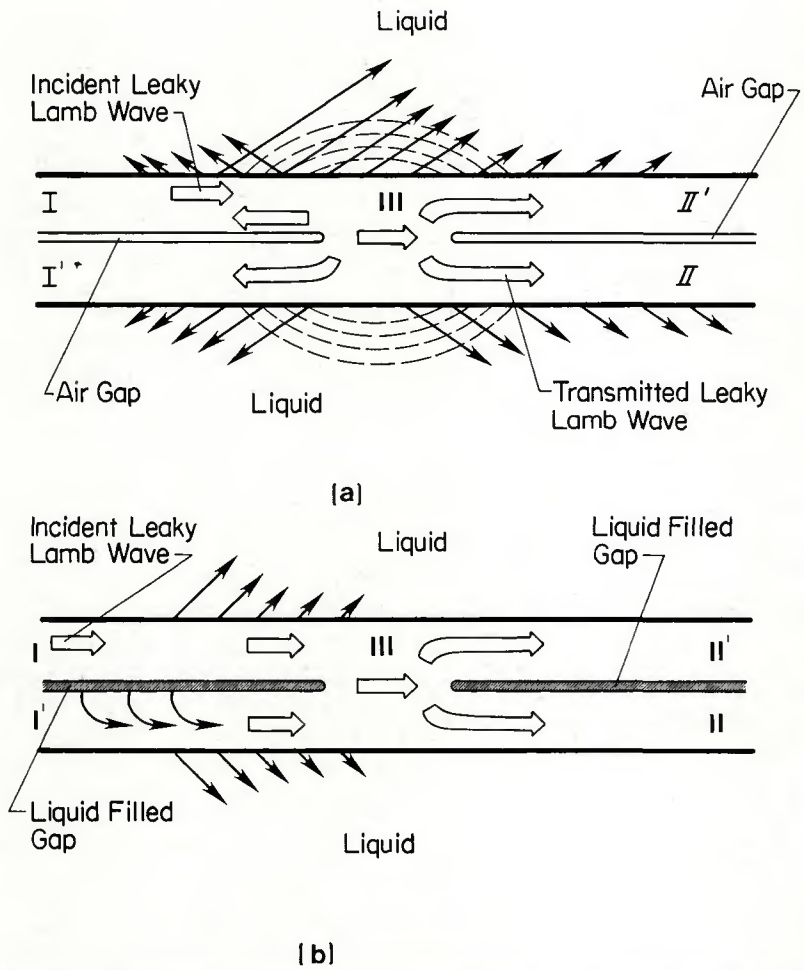

Fig. 4 — Interaction of leaky Lamb wave with aperture when sample is immersed in liquid. A — the case with an air gap between the sheets; B — coupling of waves by a liquid filled gap

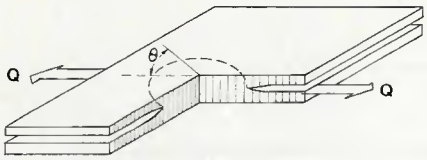

Fig. 5—Fracture mechanics model of a spot weld

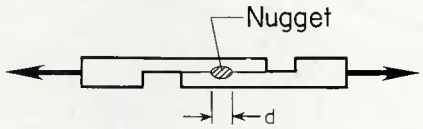

Fig. 6—Tensile test with lap shear specimen for spot weld

that bonding of the plate region I, I′, II and II′ by the liquid is not symmetrical. There is liquid only on one surface of the plate. The other surfaces are separated by air gaps. Therefore, leakage of energy to the liquid takes place from only one surface.

In the second case (Fig. 4B) (fluid-filled gap), the wave behavior changes drastically. The liquid filled gap couples the plates (I-I′ and II-II′), and the incident energy is redistributed between the I and I′ plates before it reaches the junction region III. The coupling exists when the component of the displacement of the incident wave normal to the plate surface is nonzero, which is exactly the case for the leaky wave. If the surface-normal displacement is zero, the Lamb wave does not leak energy to the liquid and cannot be excited in the plate by an ultrasonic beam incident from the liquid. When coupling exists due to liquid filling the gap, the incident wave will appear in both lower (I′) and upper (I) plates, and the transmission of the field through the junction region (III) to region II will be greatly affected. Further discussion of the coupling effect will be presented later in this paper.

Relation of Ultrasonic Data to Fracture Data

As shown above, we can determine the diameter of spot welds using ultrasonic techniques. To predict the mechanical properties, we need to determine the weld strength as a function of the weld diameter. The spot weld can fail in two ways: through the nugget (this usually occurs for weld diameters of small size), and through the base material by pulling the button outside the weld (in this case the welded sheets are torn in the vicinity of the weld).

We will limit ourselves here to consider only welds which failed through a nugget. From a fracture mechanics point of view, such spot welds can be modeled by an external circular crack in the solid layer—Fig. 5. A common mechanical test of a spot weld is a tensile test with a lap shear specimen—Fig. 6. Using the solution for the external circular crack subjected to equal and opposite shear forces of magnitude Q on the surface of the crack (Ref. 9) in an unbounded solid, and assuming shear force is applied far away from the spot, one can find analytical expressions for the stress intensity factors:

$$\frac{Q}{\pi^{3/2}a(b^{1/2})} \times\left[1-\frac{2(1+\nu-\frac{b}{a}\cos\theta)}{2-\nu}\right] \tag{5}$$

$$K_{III}=\frac{-2Q\sin\theta}{\pi^{3/2}a^{1/2}(2-\nu)b},\ \frac{a}{b}\ll 1 \tag{6}$$

The stress intensity factor is determined by:

$$\sigma_{ij}=\frac{K_n}{\sqrt{2\pi r}}f_{ij}(\alpha) \tag{7}$$

Here r, α and θ are coordinate variables, b is the distance of the point of application of the force from the center of the weld (half specimen length), a is the spot radius, and ν is Poisson's ratio.

The mode II stress intensity factor K_{II} depends on angle θ (see Fig. 5) and will be maximum at $\theta = 0°$. It equals zero when

$$\cos\theta=\frac{3}{2}\nu\frac{a}{b} \tag{8}$$

and is negative at $\theta = 90°$. The ratio

$$\frac{K_{II}(90°)}{K_{II}(0°)}=-\frac{3}{2}\frac{a}{b}\nu \tag{9}$$

is very small because in our case a/b is about 0.01. The mode III stress intensity factor K_{III} equals zero at $\theta = 0°$ and is maximum at $\theta = 90°$. The ratio

$$\frac{K_{III}(90°)}{K_{II}(0°)}=-\left(\frac{a}{b}\right)^{3/2} \tag{10}$$

for our case will be about 10^{-3}. So a test with $b \gg a$ can be considered as the test to study the second fracture mode.

In the case of an external circular crack in a plate subjected to equal and opposite shear forces on the crack surface, we can write for $K_{II}(0°)$ by analogy:

$$K_{II}=\frac{2Q\sqrt{b}}{\pi^{3/2}a^2(2-\nu)}F(a,h) \tag{11}$$

where Q can be adopted as the tension load P for the lap shear specimen, and h is the thickness of the unwelded sheets. The function F(a,h) varies only slightly when h > a, which is our case here. The estimation was made using the results of an analogous problem of an internal circular crack in a plate (Ref. 9). So we take F(a,h) = 1.

The K_{II} determines the intensity of the crack tip stress, during shear sliding (Fig. 7) of the crack surfaces over one another in a direction perpendicular to the crack edge. When the load is such that K_{II} reaches its critical level, failure occurs (the crack starts to propagate). This critical value of the stress intensity factor could be considered as the shear fracture toughness (K_{IIc}) of the material and it is the characteristic parameter of the material. It can be determined from

$$K_{IIc}=\frac{2Q_c\sqrt{b}}{\pi^{3/2}a^2(2-\nu)} \tag{12}$$

where Q_c = critical (fracture) shear load. We can point out that equation (12) can be used for shear fracture toughness measurements. Inversely, if the shear fracture toughness (material parameter) is known along with the spot weld diameter, the failure load of the spot weld can be predicted.

$$Q_c=\frac{K_{IIc}\pi^{3/2}(2-\nu)D^2}{8\sqrt{b}} \tag{13}$$

The equation (13) is valid only for the case when failure occurs through the nugget. But it was shown experimentally (Ref. 3) that the shear failure load Q_c is proportional to the squared nugget diameter also in the cases when failure occurs in the base material by pulling of a nugget outside the weld. Figure 8 also supports

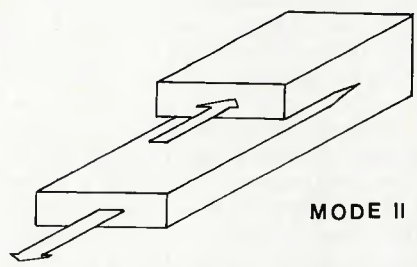

Fig. 7—Mode II of cracking (sliding of the crack surfaces)

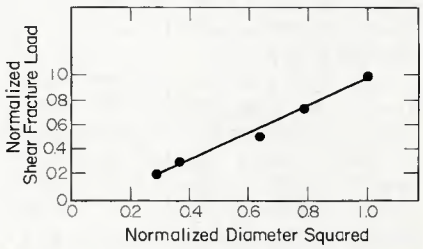

Fig. 8—Shear fracture load of spot welds versus its diameter squared (data collected from Ref. 10)

the D^2 law of equation (13). It shows the shear strength data collected from the resistance welding manual (Ref. 10) for different diameters of the spot welds. Equations (4) and (13) give an algorithm for prediction of the failure load of the spot welded specimen using ultrasonic measurements.

Experimental Technique

Spot Weld Preparation and Estimation of the Effective Diameter of the Welded Region (Nugget Diameter)

The spot welding was performed by the conventional resistance spot welding technique with 0.035 in. (0.9 mm) thick 304 stainless steel sheets. Welding regions of different diameters were obtained by changing the current, the electrode diameter, and the pressure of the electrodes on the sheet. After ultrasonic measurements, all the specimens were fractured by shear stress, and the fracture areas of the weld were analyzed with a Scanning Electron Microscope (SEM).

Failure occurred precisely along the plane of the junction between the sheets and the failed region could be clearly discerned on the sheet surface. Figure 9 shows a typical example of a SEM microphotograph of the region of the weld between the sheets after failure. The area of each welded region was measured using these microphotographs. The shape of some of the weld regions was more distorted than the one shown, and some of the welds had cavities of different sizes. The area of the cavities was excluded from the effective area of the weld. The boundary of separation between fractured and non-fractured surfaces can be clearly determined on the SEM microphotograph as shown in Fig. 10, where the fractured region is on the right side of the picture and the cavity region, where the metal was melted but not bonded, is on the left side. For very short welding times, non-welded regions can appear in the middle of the spot as shown in Fig. 11. This phenomenon can be explained (Refs. 11 and 12) by the temperature distribution (Fig. 12) on the welded interface at the initial time of the welding process. In all these cases, the effective diameter of the welded region was determined as the diameter of the equivalent circle with the same area.

Ultrasonic Measurements

Contact measurements. The contact ultrasonic measurements were performed at 2.1 MHz, which yields such a value of $K_t h$ that reflection coefficient R^q_1 in equation (1) is close to zero. To excite Lamb waves, we used plexiglass wedge transducers with a variable incidence angle (Ref. 2). A longitudinal ultrasonic wave is excited in the plexiglass wedge using interchangeable rectangular piezoceramic plates. The thickness of the piezoceramic plates is selected in accordance with the required frequency. The angle of incidence of the ultrasonic beam to obtain the required Lamb wave is selected from the familiar expression (Refs. 4, 5).

$$\Theta = \arcsin V_o/V \qquad (14)$$

where V_o is the velocity of the longitudinal wave in the wedge material and V is the phase velocity of the Lamb wave. The velocity of the longitudinal wave in the wedge material was measured after stress relief and was found to be $V_o = 2.73 \times 10^3$ m/s. The measurements were performed with the S_o mode, which was excited in the 0.9 mm (0.035 in.) thick sheet. The transducer angle was preset close to the calculated value by smoothly changing the incidence angle until the maximum amplitude of the excited wave was obtained. The incidence angle Θ_{S_o} at 2.1 MHz was found to be 34°. We used sufficiently narrow spectrum bursts so that no extraneous modes were induced in the sheets, and it was possible to selectively excite and receive the required mode (mode S_o in the case under study).

The method of measurement is illustrated schematically by Fig. 1A. In accordance with Fig. 2, the transmitter is situated in region I and the receiver in region II. The amplitude of the transmitted S_o mode is obtained between two transducers placed on a single unwelded 0.9 mm (0.035 in.) thick sheet—Fig. 1B. The distance between the transducers (6-8 cm/2.36-3.15 in.) was selected to be the same as in the measurements with welded specimens. This made it possible to take into account the sensitivity of the transducers and the transmission losses in the sheet due to absorption and spread-

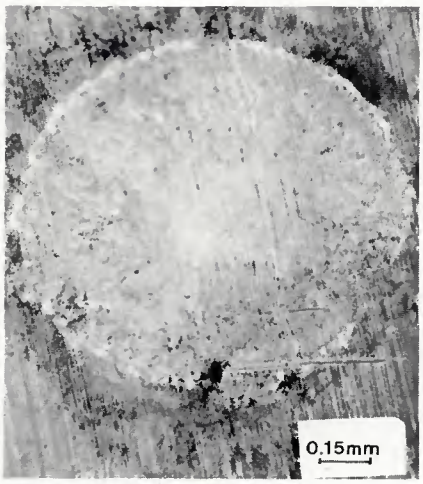

Fig. 9—SEM photomicrograph of the welded region after failure

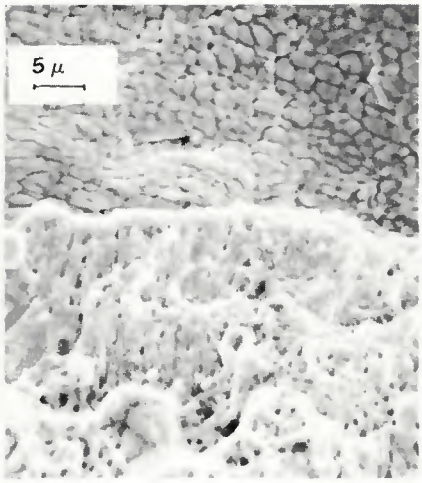

Fig. 10—SEM photomicrograph of the boundary of separation between fractured and non-fractured (left) regions

Fig. 11—SEM photomicrograph for weld with very short welding time

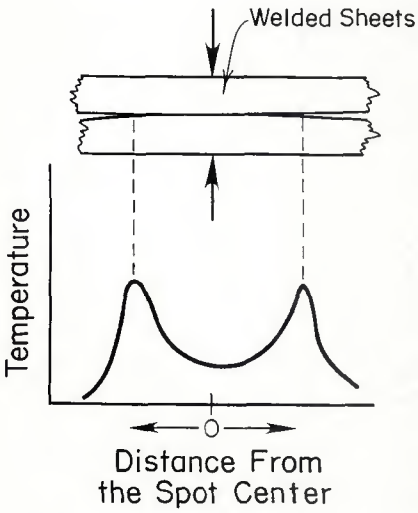

Fig. 12—Schematic explanation of the phenomenon shown in Fig. 11, by temperature distributions at the initial time of the welding process

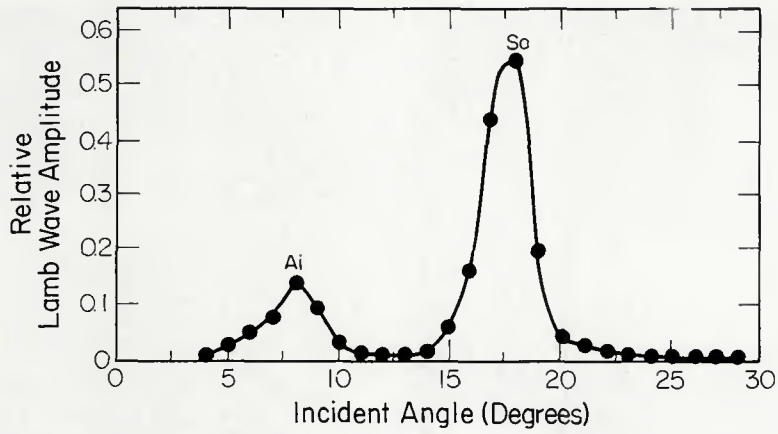

Fig. 13 — The amplitude of the received ultrasonic signal as a function of the incident angle Θ in immersion measurements

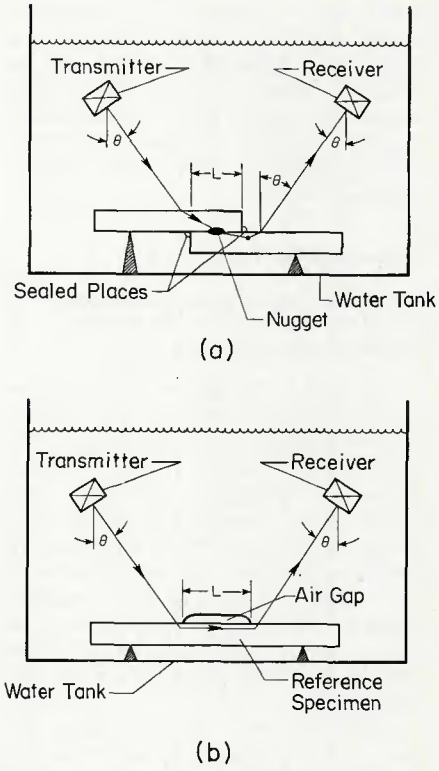

Fig. 14 — Schematic explanation of the immersion method of measurement

ing of the ultrasonic beam. Such a normalized quantity can, by definition, be taken as the amplitude coefficient of transmission through the welded region. It can be shown that the received electric signal is proportional to the amplitude of the transmitted S_0 mode which, by definition (Ref. 6), is given by the expression $T = \sqrt{t}$, where t is the energy-flux transmission coefficient. The wedge transducers are unidirectional; therefore, the signals reflected from the plate edges are not recorded by the receiving transducer. The diameter of the incident beam is about 1 cm (0.39 in.), which significantly exceeds the dimensions of the weld region, and hence the incident wave can be treated as plane.

Immersion measurement. Let an ultrasonic beam be incident on a plate immersed in liquid. If the incident angle selected is according to equation (14), where V_0 is the wave velocity in the liquid, the leaky Lamb wave with phase velocity V is excited in the plate. That excited Lamb wave reradiates (leaks) elastic energy at the same angle to the liquid from both surfaces of the plate and can be received by the receiving transducer.

The amplitude of the received ultrasonic signal as a function of the incident angle Θ is shown in Fig. 13. The optimal working angle was chosen as 18°, according maximum sensitivity for the S_0 mode.

The immersion ultrasonic measurements were performed at the same frequency and for the same samples which were studied with contact techniques. The immersion method of measurement is shown schematically in Fig. 14.

The tips of the lap region L were sealed, as shown on Fig. 14A, to exclude coupling between sheets through the water gap. The incident ultrasonic beam excited the S_0 leaky Lamb mode in the upper sheet. This mode reaches the nugget and is partially transmitted to the lower sheet. From this lower sheet, elastic energy is reradiated to the upper liquid half space and is received by the receiving transducer. The amplitude of the leaky S_0 mode transmitted through the weld was normalized by the magnitude of the reference signal, as shown in Fig. 14B. This normalization excludes transducer sensitivity effect and effects of transmission losses due to leakage and spreading of the ultrasonic beam. In the region of overlap L (Fig. 14A), sealed welded sheets make contact with the liquid on one side only. Therefore, we uncoupled one surface of the reference specimen from the liquid by an air gap (Fig. 14B) to avoid leakage of elastic energy to the water from one surface of the specimen on the acoustic path L.

Some experiments were performed to study resonance effects in the welded region using spectroscopic techniques. Short ultrasonic pulses, normally incident from the liquid onto the weld, were used. We performed spectral analysis of signals reflected from the welded plates. The broadband focus Harisonic transducer (central frequency 5.3 MHz, F = 3.5 MHz at −3dB) and digital spectroscopic analysis (Refs. 13 and 14) were used in these experiments.

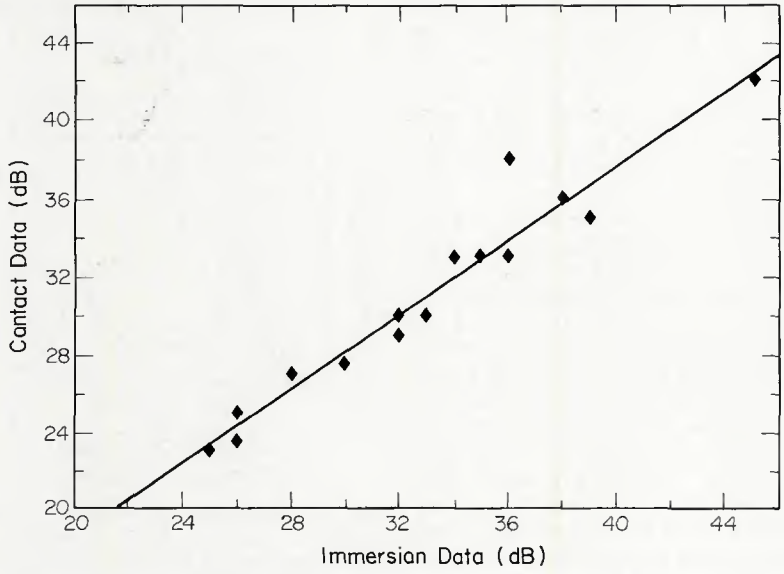

Fig. 15 — Comparison of the immersion and contact data

Strength Measurements

The specimens were prepared as shear lap specimens (Fig. 6) for testing under

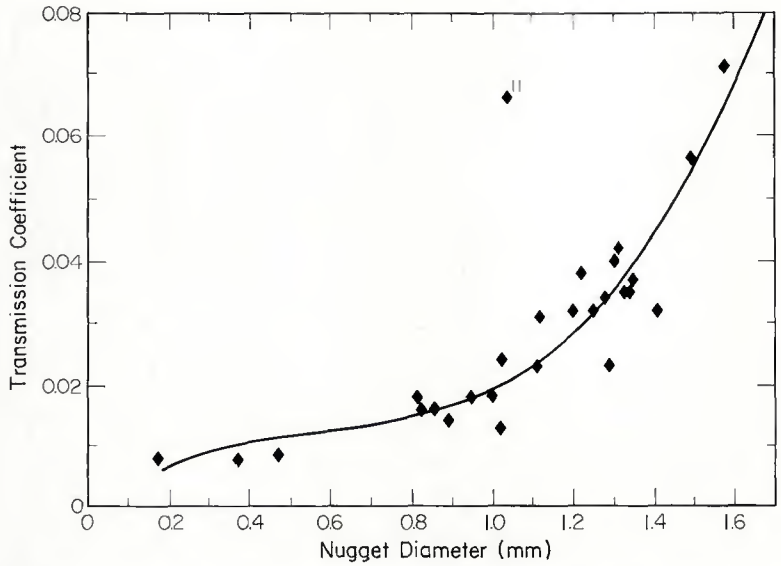

Fig. 16 — Transmission coefficient of the mode S_0 through the spot weld region as function of the mean diameter of the welded region

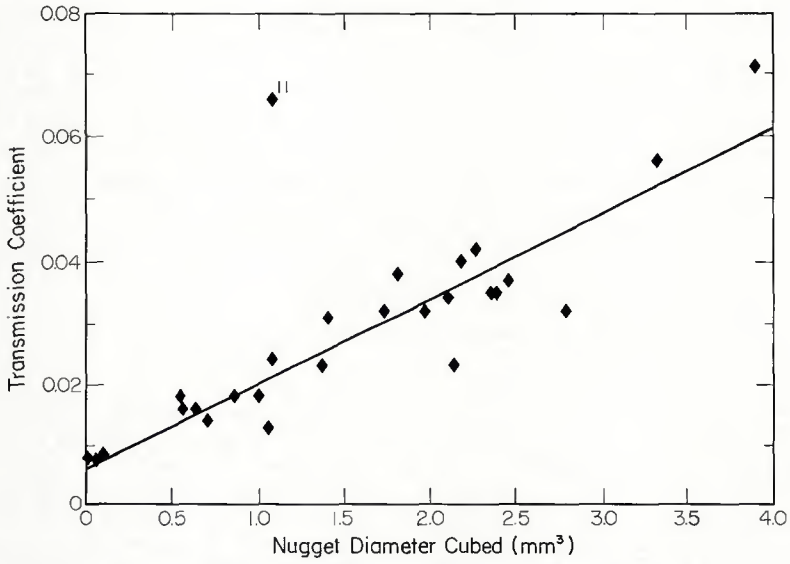

Fig. 17 — The same as in Fig. 16, only transmission data versus diameter cubed

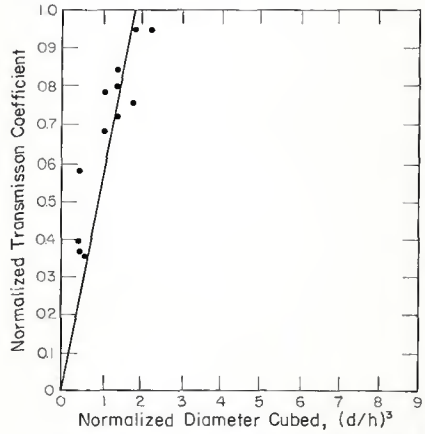

Fig. 18 — Data for small welded diameters measured by immersion technique without sealing of the air gap between sheets

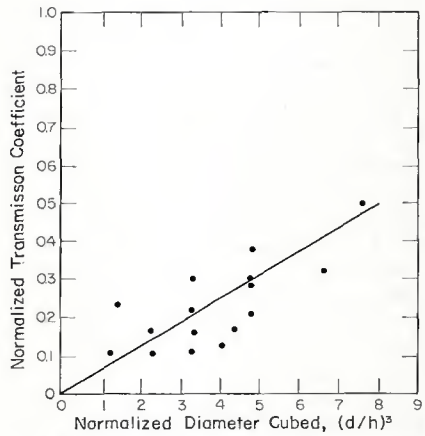

Fig. 19 — Data for large welded diameters measured at the same conditions as data for Fig. 18

tensile load on an Instron machine. Special care was taken to minimize the effect of misalignment between the axis of the nugget and the tensile axis. The thickness of both end sections of the specimens were the same as the thickness of the welded region to prevent bending moments.

Results and Discussion

The Lamb wave transmission coefficient was measured for all welded specimens both by contact and immersion techniques. The air gap between sheets was sealed and therefore is not filled with water. All immersion and contact data received are compared in Fig. 15. The results compare quite well, excluding a systematic shift of about 1.5 dB of immersion from contact data. Possibly, this shift can be explained by different sealings of the samples and reference used in immersion measurements.

Transmission coefficients of S_0 Lamb wave versus nugget diameter are shown in Fig. 16. Experimental data are fitted by a third order polynomial. The scattering of the data from the fitted curve in the range ± 0.1 mm (± 0.004 in.) is comparable with the precision of effective diameter measurements using microphotographs of fractured specimens. This scatter is larger than the scatter of previous (Ref. 1) data from the d^3 curve. This is explained by our wish to have a large variation in nugget diameter, and thus most of the welds were not made in an optimal condition. This results in shape distortions of the welded region and cavities in it. That makes it difficult to find the exact effective area of the weld. Note that welds studied in Ref. 1 had no cavities at all.

Data from Fig. 16 are replotted versus d^3 in Fig. 17. In these coordinates, the results behave reasonably linearly which supports the $T \sim d^3$ theoretical relation. The separate set of samples was measured (Ref. 15) by an immersion technique without sealing of the air gap between sheets, and so the gap was filled with water. Data (Ref. 15) are shown separately for small (Fig. 18) and large (Fig. 19) welded diameters. Here the amplitude of the transmitted signal is strongly affected by coupling through liquid. For small welded regions, the thickness of the gap is greater, and liquid penetrated it more easily. In the case of large welded regions, the welded sheets touched one another more closely, and liquid penetrated into a smaller area. The instability of this effect explains the larger scatter in the data.

The effect of coupling was studied in nonwelded liquid coupled sheets in the

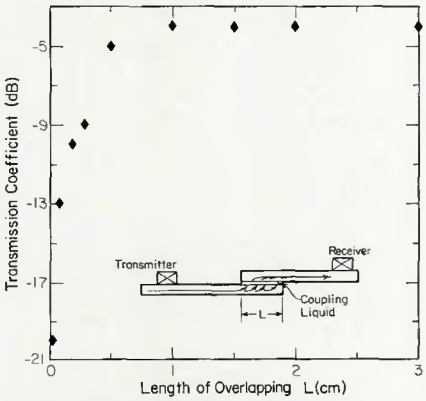

Fig. 20—The experimental configuration and experimental results for S_o Lamb wave transmission through liquid coupling layer

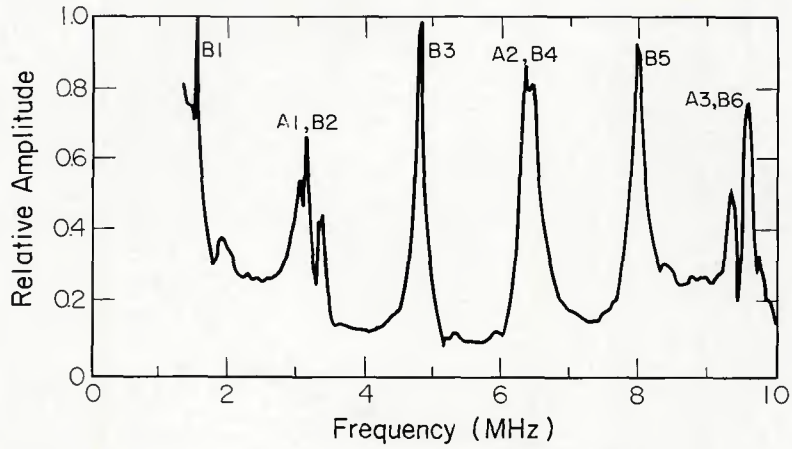

Fig. 21—Reflected spectrum from spot weld of large diameter

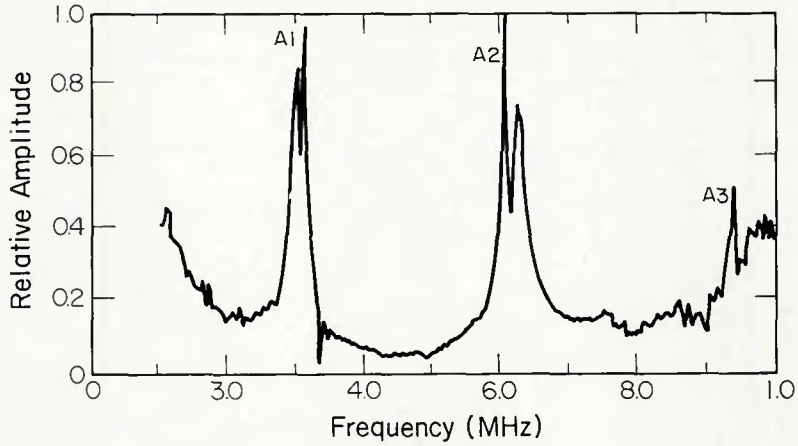

Fig. 22—Reflected spectrum from spot weld of small diameter

same conditions as used for contact measurements with welded samples. The experimental configuration and experimental results are shown in Fig. 20.

The amplitude of the transmitted signal is plotted as a function of the length of the liquid coupling region. When the coupling length is of order 0.6-1 cm (0.24-0.40 in.), transmission losses reach their minimum value of order −4 dB. This is very close to the minimally possible theoretical loss of −3 dB. These experimental data show that for given working conditions, the tips of the lap regions have to be sealed during the immersion testing procedure.

We attempted to use also a spectroscopic technique for nugget diameter measurements. Here will be shown only preliminary results, which show qualitatively that such application is possible.

When a pulsed ultrasonic signal is normally reflected from a plate, it consists of two parts: the forward part directly reflected from the top surface of the plate, and the following reverberating part of the signal, which is formed by multiple reflection of the elastic energy in the plate from its surfaces. In the measurements discussed below, the directly reflected part of the signal was eliminated by a digital gating.

The spectrum of the reverberating part of the pulse reflected from the 4 mm (0.16 in.) diameter spot weld is shown in Fig. 21. There are two sets of resonances in the reflected spectrum. The first set labeled B1, B2, B3, etc., is identified with thickness resonances of the welded region:

$$f_n = \frac{v_e \cdot n}{2H}$$

where f_n is the frequency of resonance number 'n', v_e is the velocity of the longitudinal wave in the sheet and H is the thickness of the welded region ($H = 2h - \delta$ where h is the original thickness of the welded sheets and δ is the thickness change during the welding process). The second set labeled A1, A2, A3 is identified with resonances in the upper sheet of thickness h. These last resonances appear because the diameter of the incident beam is larger than the diameter of the nugget. Due to interference between close frequency components A1-B2, A2-B4 and A3-B6, this part of the spectrum is distorted. Ratios of the spectral amplitudes A-B carry information on relative dimensions: nugget diameter—incident beam diameter. The reflected spectrum (Fig. 22) from the smaller welded region (D = 1.6 mm/0.06 in.) is drastically changed. The first set of resonances BN no longer appears. The diameter of the welded region is too small for excitation of the thickness resonances in this region.

Only coupling oscillations in the upper and lower sheets are recognized. The welded region couples oscillations of the upper and lower plates resulting in frequency splitting of the resonances (Fig. 22) and beating of the signal in time—Fig. 23. This is schematically explained in Fig. 24. When the diameter of the spot weld is small compared to the diameter of the incident beam, only a small part of the incident energy is transmitted into the lower sheet. A certain period of time (the transition time) is required for the formation of the resonance in the lower sheets. The reflected signal is mostly formed by reflection in the upper sheet, and only a small part of the vibration energy in the lower sheet returns to the upper sheet and affects the reflected signal.

But it is known that in coupled systems, the oscillation energy is transferred from one part of the system to the other through the coupling. During the decrease of vibration in the upper sheet (left part of the time domain in Fig. 23) the vibration increases in the lower sheet. Afterwards the vibration energy starts to be transferred back from the lower to the upper sheet (middle part of the time domain in Fig. 23), and the amplitude of the reflected signal starts to grow.

The intensity of the beats and the character of the frequency splitting of the resonance peaks are functions of the coupling coefficient which are determined by the diameter of the spot weld. Inversely, these characteristics can be used to estimate the diameter.

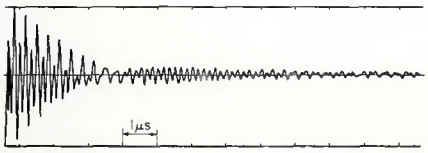

Fig. 23 — Beatings of the reflected signal in the time domain for a small spot diameter

Fig. 24 — Schematic explanation of coupling wave through small welded region

Therefore, diameters of spot welds can be measured with spectroscopic techniques in two ways: for large diameters by comparison of the amplitudes of thickness resonances for the weld region and the upper sheet, and for small diameters by splitting of the resonances and beating in the time domain.

After ultrasonic measurement, the specimens were fractured with a shear tensile test (some weak specimens were broken inadvertently during measurement). The results of the normalized shear fracture load versus nugget diameter squared are shown in Fig. 25. The solid line is the least square fit to the data and the broken line is the behavior predicted by equation (13). The data for specimens 4, 17 and 26 lie away from the fitted line. These were specimens with cavities. The effective diameters of the welded regions, determined without exclusion of the area of the cavities from the overall area, are shown as white triangles. Possibly in this case the cavities do not change the stress concentrations on the crack ends and therefore do not affect the fracture load. A SEM microphotograph of the weld region for the sample 26 is shown in Fig. 26. The ultrasonic data for specimen 11 lies away from the d^3 curve in Figs. 16 and 17, but is well fitted in the strength data, so there was no mistake in determination of the weld diameter. Possibly during contact ultrasonic measurements, a small amount of the coupling liquid penetrated between the welded sheets, changing the amplitude of the transmitted signal.

The method for failure load prediction is illustrated schematically in Fig. 27, where from the measured Lamb wave transmission coefficient the nugget effective diameter cubed, D^3_{eff}, was determined. The slope of the correlation line depends on the frequency of the measurements, the plate thickness and the material parameters. Based on the diameter data, the fracture load can be found as is shown in the lower figure — Fig. 17. The slope of the correlation line here depends on metallurgical parameters of the welded region.

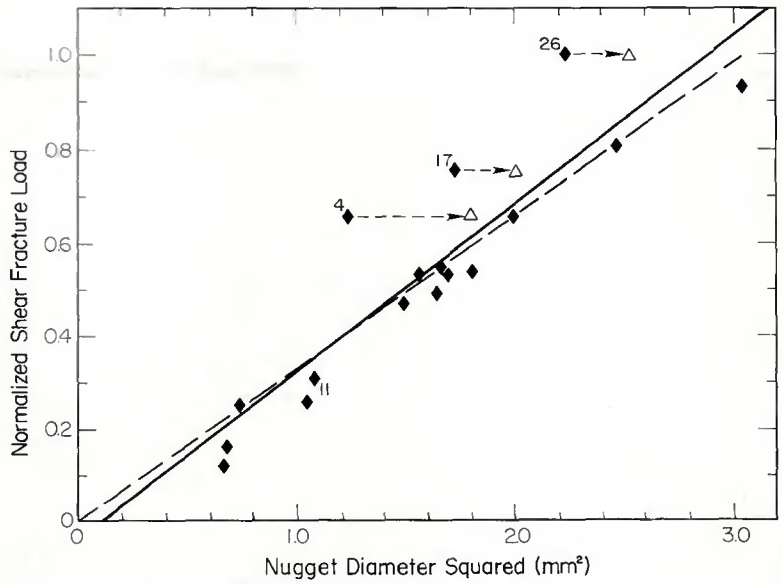

Fig. 25 — Normalized shear fracture load versus mean diameter of the welded region. The solid line is the least square fit and the broken line is the behavior predicted by theory. The data were normalized by dividing on maximum failure load achieved in this group of experiments

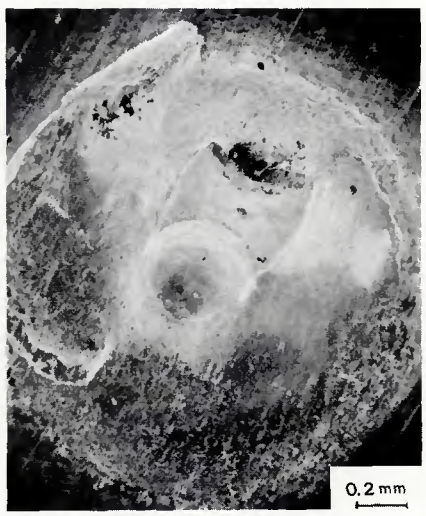

Fig. 26 — A SEM photomicrograph of the weld region for the sample with cavity

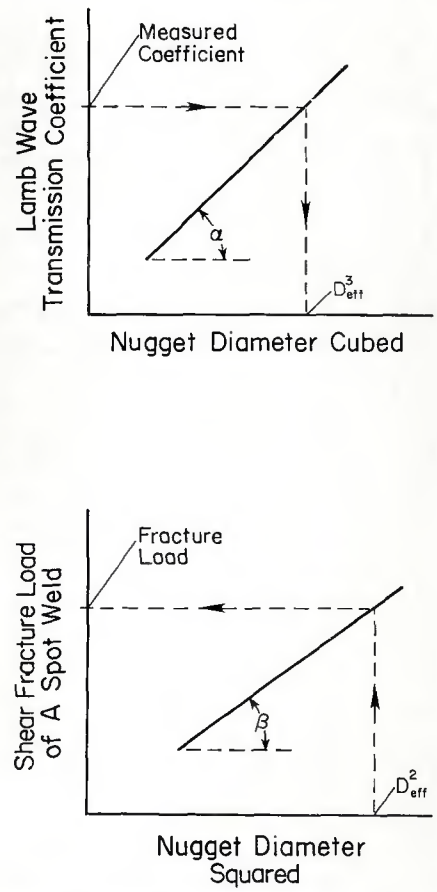

Fig. 27 — Schematic illustration of the method for failure load prediction

Conclusion

In this work, we introduce a new concept for nondestructive evaluation of spot welds. This concept is based on ultrasonic measurement of the spot weld diameter (diameter of the nugget) which is then used for failure load prediction.

Two ultrasonic techniques were used: Lamb waves and ultrasonic spectroscopy with longitudinal waves. Our analysis shows that the Lamb wave transmission coefficient is proportional to D^3, when D is the mean diameter of the welded region (nugget diameter). The above relation allows one-to-one determination of the mean diameter of the nugget on the basis of the amplitude of the transmitted

signal. This relation was checked experimentally by contact and immersion measurements. Both results have good agreement with the theoretical prediction. The spectroscopic technique also shows some possibilities for spot diameter estimation: for large diameters, by comparison of the amplitudes of thickness resonances for the weld region and the upper sheet, and for small diameters, by splitting of the resonances and beating in the time domain.

To predict the mechanical properties of the spot weld we applied a fracture mechanical model, considering the spot joint as an external circular crack in the solid layer. This model predicts that the failure load is proportional to the squared nugget diameter. While the fracture mechanical model is valid only when the nugget size is small and the weld fails through the nugget, it was established experimentally that the shear failure load related to the squared nugget diameter, also for large nugget diameters when failure occurs in the base metal, by pulling a welded button outside the weld. Using this relation between failure load and spot weld diameter, the failure load can be determined on the basis of ultrasonic data. The experimental data show good agreement with the theoretical predictions.

Acknowledgment

The authors wish to thank Professor C. Popelar for a fruitful discussion of the fracture mechanics model and Dr. A. Jungman for contributions to the spectral analysis measurements.

References

1. Rokhlin, S. I. and Bendec, F. 1983. *J. Acoust. Soc. Am.* 73: 55–60.
2. Bendec, F., Perec, M., and Rokhlin, S. I. 1984. *Ultrasonics* 22: 78–84.
3. Rokhlin, S. I., Mayhan, R. J., and Adler, L. June, 1985. Materials Evaluation.
4. Auld, B. A. 1973. *Acoustic Fields and Waves in Solids,* Vol. II. Wiley-Interscience, New York.
5. Viktorov, I. A. 1967. *Rayleigh and Lamb Waves.* Plenum, New York.
6. Rokhlin, S. I. 1981. *J. Acoust. Soc. Am.* 69: 922–928.
7. Rokhlin, S. I. 1979. *Int. Adv. Non-destr. Test.* 6: 263–285.
8. Collin, R. E. 1960. *Field Theory of Guided Waves.* McGraw-Hill, New York.
9. Kassir, M. K., and Sih, G. C. 1975. Three-dimensional crack problems, *Mechanics of Fracture,* Vol. 2. Edited by G.C. Sih, Noordhoff Int. Publ., Leyden.
10. *Resistance Welding Manual,* 1969. Vol. I, E. J. D. Vecchio, editor. Published by Resistance Welder Manufacturers' Assoc., Philadelphia, p. 131.
11. Greenwood, J. A., and Williams, J. B. 1958. *Proc. Royal Soc.* 264A: 13.
12. Greenwood, J. A. August 1960. Welding Research, B.W.R.A.: 316–322.
13. Adler, L., and Achenbach, J. D. 1980. *J. Nondestr. Eval.* 1: 87–99.
14. Fitting, D. W., and Adler, L. 1981. *Ultrasonic Spectral Analysis for Nondestructive Evaluation.* Plenum Press, New York.
15. Chang, M. C. 1983. M.S. thesis. Department of Welding Engineering. The Ohio State University.

—A Reminder to Authors—

Application forms for presentation of technical papers in the 1986 AWS Convention Professional Program must be postmarked no later than **August 1, 1985.** Be sure to send your application forms and 500–1000 word summaries in on time to ensure consideration for the 67th Annual AWS Convention, to be held April 13–18, 1986, in Atlanta, Ga.

A tear-out Author Application Form can be found in the May, 1985, issue of the *Welding Journal.* For additional applications, contact: Mr. T. P. Schoonmaker, Technical Papers Editor, American Welding Society, P. O. Box 351040, Miami, FL 33135; telephone (305) 443-9353.

WRC Bulletin 301
January 1985

A Parametric Three-Dimensional Finite Element Study of 45 Degree Lateral Connections
By P. P. Raju

This bulletin contains a summary of three-dimensional finite element studies carried out on four lateral configurations subjected independently to internal pressure, external in-plane moment on the nozzle, and external in-plane moment on the run pipe. Stress indices for various critical regions are summarized.

Publication of this report was sponsored by the Task Group on Laterals that reported to the Subcommittee on Reinforced Openings and External Loadings and the Subcommittee on Piping Pumps and Valves of the Pressure Vessel Research Committee of the Welding Research Council.

The price of WRC Bulletin 301 is $14.00 per copy, plus $5.00 for postage and handling. Orders should be sent with payment to the Welding Research Council, Room 1301, 345 E. 47 St., New York, NY 10017.